ACS PHYSICAL CHEMISTRY Au
AN OPEN ACCESS JOURNAL OF THE AMERICAN CHEMICAL SOCIETY

pubs.acs.org/physchemau

Perspective

Growth of Lead Halide Perovskite Nanocrystals: Still in Mystery

Narayan Pradhan*

Cite This: *ACS Phys. Chem Au* 2022, 2, 268–276

Read Online

ACCESS | Metrics & More | Article Recommendations

ABSTRACT: Lead halide perovskite nanocrystals with different halide ions can lead to color-tunable emissions in visible window with near-unity photoluminescence quantum yields. Extensive research has been carried out for optimizing the synthesis of these nanocrystals for the last 6 years, and thousands of research papers have been reported. However, due to the ionic nature, these nanocrystals formed instantaneously and hence, their growth kinetics could not be established yet. In most of the reactions, the formation mechanism typically followed one reaction for one size or shape principle, and their dimension tuning was achieved predominantly with thermodynamic control. There is no clear evidence yet on the decoupling growth from nucleations and monitoring their growth kinetics. Hence, the progress of understanding the fundamentals of crystal growth faced road blocks for these halide perovskite nanocrystals. Keeping eyes on all such reports on one reaction for one size and one reaction for tunable size of the most widely studied $CsPbBr_3$ nanocrystals, in this perspective, details of their size tunability are analyzed and reported. In addition, comparison of the classical mechanism, obstacles for establishing secondary growth, and possible road maps for controlling the kinetic parameters of formation of these nanocrystals are also discussed.

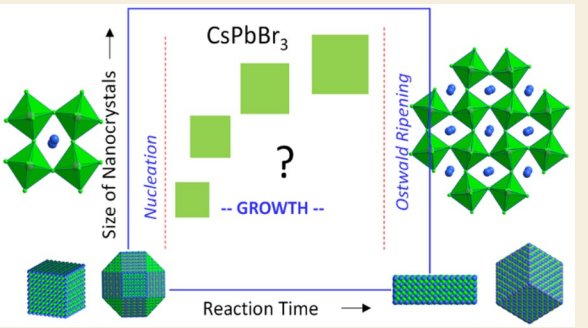

KEYWORDS: *perovskite nanocrystals, growth kinetics, polyhedral nanocrystals, $CsPbBr_3$, nanocubes*

How do lead halide perovskite nanocrystals nucleate and grow? Despite several successes achieved in designing size- and shape-modulated halide perovskite nanocrystals, basic fundamentals of their formation still remained elusive.[1−8] In most of the leading reports, formation of each size or shape of these nanocrystals typically required a separate reaction.[1,8−13] This is because of the adopted ice-cool approach which remained essential for obtaining phase-stable and bright emitting nanocrystals. These lead halide perovskite nanocrystals soon after their first report swiftly emerged as the leading optical emitters in the field and provided an opportunity to obtain all three leading colors, red-green-blue, with near-unity photoluminescence quantum yield (PLQY).[10,12,14−30] Initially, only six faceted cubes and platelets were reported but later extended to several polyhedral shapes[4,25,31,32] without compromising their brightness. However, all of these successes were achieved with varying reaction parameters and reagent modulations, but not with the control of their growth kinetics. In fact, despite thousands of reports, there is no growth kinetics established until now that would provide the pathway of growth versus monomer concentration or size variation in a standard reaction time protocol. The classical mechanism of nanocrystal growth, which typically follows the La Mer model,[33] was mostly established for covalent nanocrystals like metal chalcogenides. Instead, for the ionic nature of the A-site ion bonds, these lead halide perovskite nanocrystals form instantaneously, and hence ion-adsorption-based successive growth could not be established.[7] Hence, the question arises whether monitoring the growth kinetics would be practically possible or remain a mystery. Slowing down the reaction and controlling secondary growth remained critically important for studying the growth doping and facet directive growth, shelling of these materials, and also obtaining heterostructures, and all of these processes were no successfully established yet.[2,3] As this is a fundamental issue and critically important for understanding the growth of halide perovskite nanocrystals, details of the established facts on formation of size and shape variability of nanocrystals, the impact of temperature, precursors, and ligands for dimension tunability and controlling reaction parameters for initiating secondary growth remained important. Studying all of these parameters from different established reactions, their details of formation and possible establishment of growth kinetics in comparison with classical mechanism are analyzed and reported in this perspective. Moreover, several possible pathways to establish the kinetics are also discussed.

Limiting the discussion only to $CsPbBr_3$ nanocrystals, which are most widely studied among all lead halide perovskite

Received: January 3, 2022
Revised: February 6, 2022
Accepted: February 7, 2022
Published: February 21, 2022

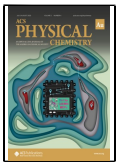

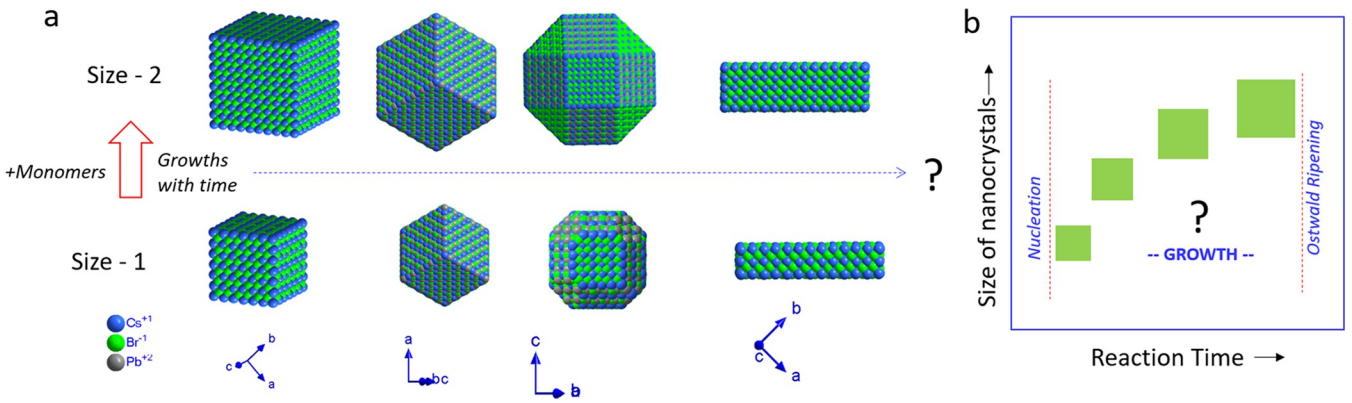

Figure 1. (a) Schematic of atomic models showing the growth of perovskite nanocrystals from one size to another with progress of the reaction. Models show different polyhedral 3D $CsPbBr_3$ nanocrystals (6, 12, and 26 faceted) and platelets having different facets. The approach here is expected from a classical nanocrystal growth model. (b) Possible size versus reaction time plot. The question mark indicates the unknown growth scale of these nanocrystals.

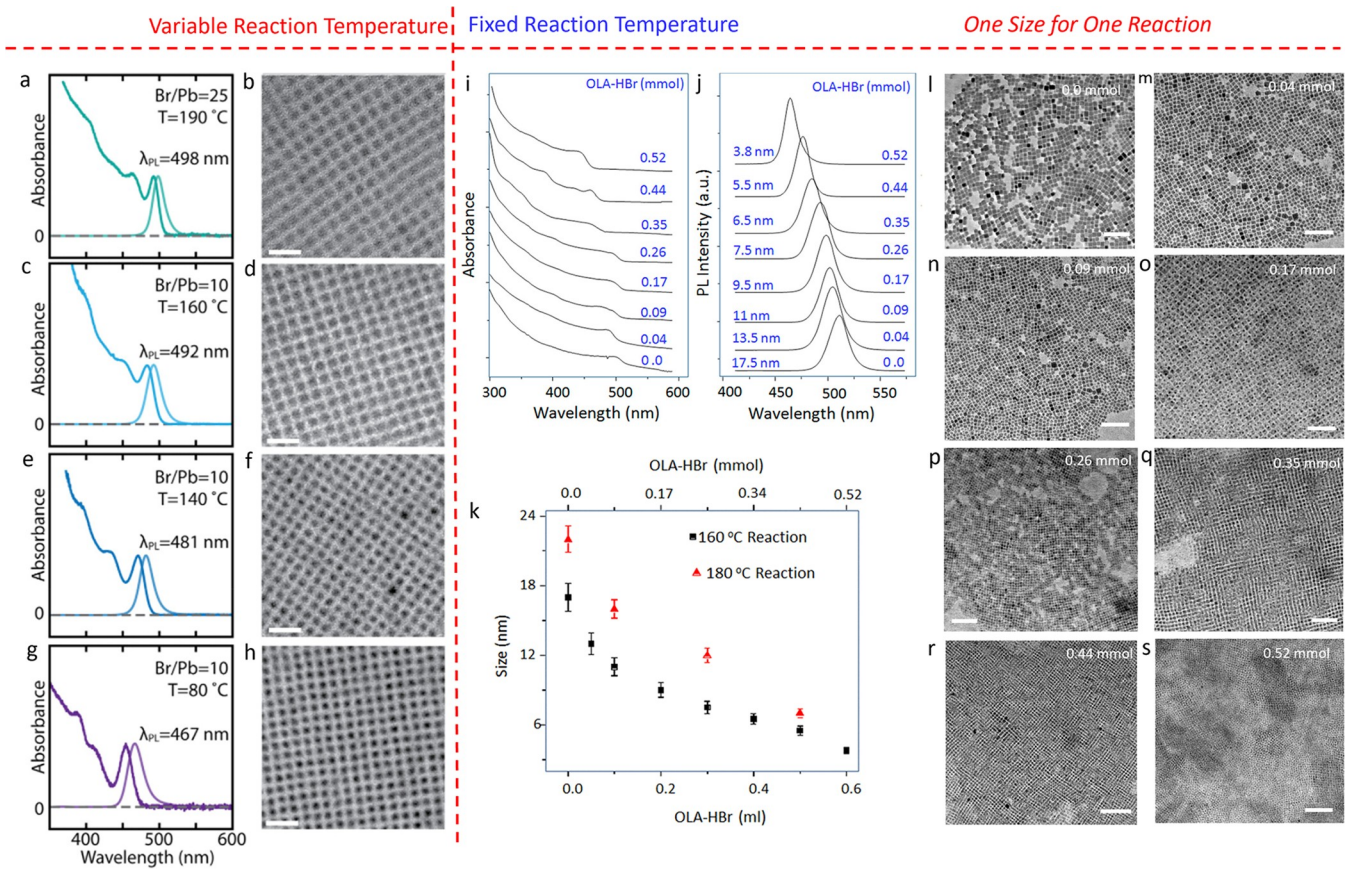

Figure 2. (a,c,e,g) Absorption and photoluminescence spectra and (b,d,f,h) corresponding TEM images of $CsPbBr_3$ nanocrystals obtained at different reaction temperatures with a Br to Pb ratio = 10-25. Scale bar for each case is 20 nm. Reproduced from ref 11. Copyright 2018 American Chemical Society. (i,j) Absorption and PL spectra of different sized $CsPbBr_3$ nanocrystals obtained with different OLA-HBr added in the reaction system. (k) Plot of size of $CsPbBr_3$ nanocrystals versus OLA-HBr concentration. (l–s) TEM images of $CsPbBr_3$ nanocrystals obtained with different concentration of added OLA-HBr. In each case, the concentration of added OLA-HBr is mentioned. Scale bar for each case is 100 nm. Reproduced from ref 34. Copyright 2018 American Chemical Society.

nanocrystals, size tuning of their isotropic 3D shapes in cubes, dodecahedra, rhombicuboctahedra, and 2D-shaped platelets was the focus. Standard growth protocol from one size to another retaining their shapes is depicted schematically in Figure 1, in which atomic models of different shapes are presented in Figure 1a and the assumed classical growth process is shown in Figure 1b. From different literature reports, it is further revealed that sizes of $CsPbBr_3$ nanocrystals are typically governed by varying the reaction temperature and halide concentration.[11,12,22,32,34−39] Figure 2a–h presents a typical case of size-tunable $CsPbBr_3$ nanocrystals from 3.7 to 9.5 nm having a fixed Pb/Br ratio and with varying reaction temperatures. This pioneering work was reported by Son and co-workers in 2018.[11] They also reported that with increasing halide [Br^-]

https://doi.org/10.1021/acsphyschemau.2c00001
ACS Phys. Chem Au 2022, 2, 268−276

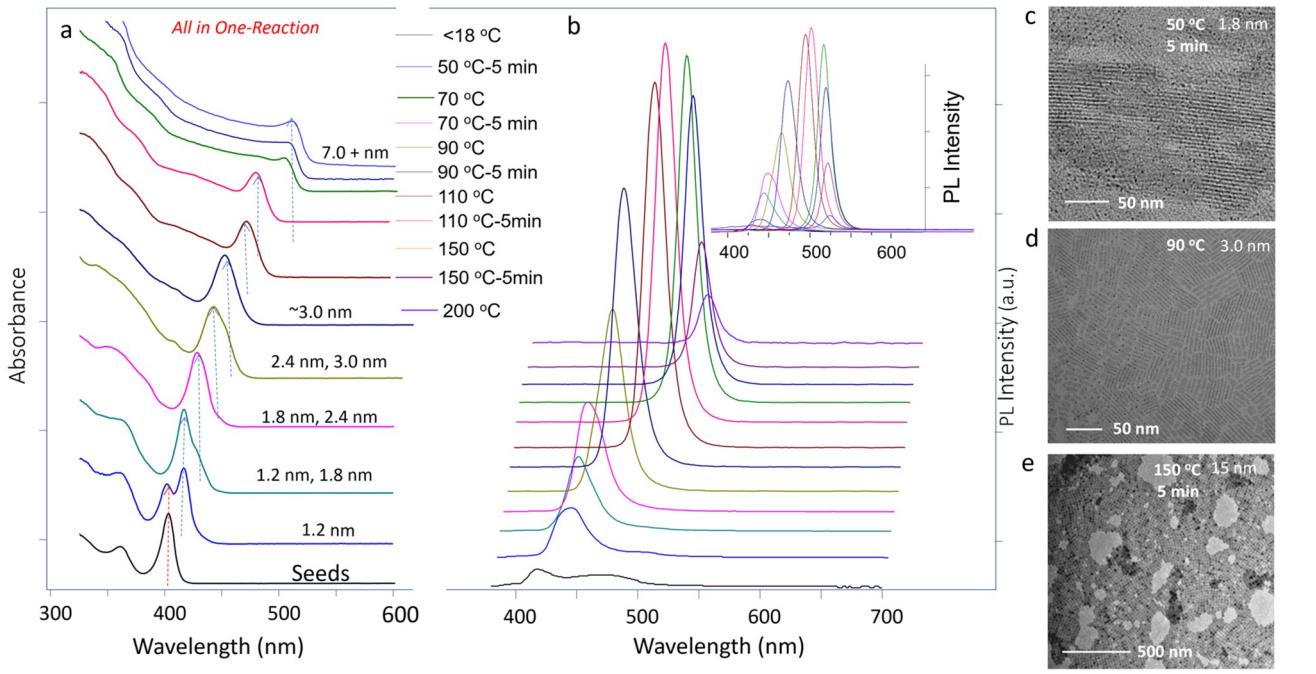

Figure 3. $CsPbBr_3$ nanocrystals obtained in a single reaction and with temperature variation using seed cluster injection method. (a) Successive absorption spectra obtained with an increase in reaction temperature at different time intervals and (b) corresponding PL spectra. Inset shows the overlapped PL spectra obtained with almost the same amount of samples collected from the reaction. Excitation wavelength is 350 nm. (c–e) TEM images representing wire/belt-like thinner and longer nanostructures, rectangular belt-like nanostructures, and cube-shaped $CsPbBr_3$ nanocrystals obtained at different stages of the reaction. Reproduced from ref 40. Copyright 2018 American Chemical Society.

concentration, the size of $CsPbBr_3$ decreases even at a fixed reaction temperature. This work also stated that the size variations were thermodynamically controlled rather than followed the kinetic model. Typically, this remained an unconventional pathway in comparison to traditionally reported quantum dots. Absorption features of these nanocrystals obtained in a halide-rich environment supported their strong quantum confinements and remained unique among all such reports. Prior to this work and in same year, Dutta et al. reported the alkyl ammonium bromide (OLA-HBr) concentration variable size variation of $CsPbBr_3$ nanocrystals.[34] In this case, the authors also observed that increasing ammonium bromide concentration reduced the size of the nanocrystals. Whereas the temperature variation was established as the key approach, this was the first report in which OLA-HBr helped with size variation even at a constant reaction temperature. Figure 2i,j presents the absorption and photoluminescence spectra of OLA-HBr variable concentrations of $CsPbBr_3$ nanocrystals. Although these nanocrystals were synthesized at 180 °C, at a different reaction temperature of 160 °C, similar OLA-HBr variable size tuning observations, but in a different size regime, were also observed. Figure 2k presents the plot of the amount of OLA-HBr versus the size of $CsPbBr_3$ nanocrystals at 180 and 160 °C. These results also suggest that with an increase of reaction temperature, the size of the obtained $CsPbBr_3$ also increases. Representative transmission electron microscopy (TEM) images of different nanocrystals obtained at the constant temperature at 180 °C and with OLA-HBr variation are presented in Figure 2l–s, and in each panel, the amount of added OLA-HBr is mentioned. Both of these results suggested that temperature and halide concentration played a crucial role in size tuning of $CsPbBr_3$ nanocrystals, although in one case Zn–Br and in another case OLA-HBr was used in respective synthesis methods.

However, none of these two cases showed the kinetics models of nanocrystal growth, in which size tunability could be achieved with progress of reaction time. To retain high PLQY, these reactions were immediately quenched. Even though halide-rich reaction systems restrict the phase change during annealing, the final size of these nanocrystals was immediately achieved soon after injection of the Cs(I) precursor. Hence, with variation of either reaction temperature or halide concentration, the size tunability followed here the one size from one reaction principle, and this is primarily thermodynamically controlled.

In another case, the impact of thermal annealing on the shape/size of $CsPbBr_3$ nanocrystals was reported, in which smaller sized nanocrystals were transformed into larger sizes with an increase of the reaction temperature.[40] It was started with quasi-spherical-type particles being transformed first to belt/wire-type nanostructures and being further transformed into platelets and cube nanocrystals. These nanostructures were synthesized by injecting seed clusters, which were initially prepared at room temperature, and the shape transformations were observed with annealing as well as an increase of reaction temperature. Interestingly, a step growth of ~1.2 nm thickness was reported during the progress of the reaction. Figure 3a presents successive absorption spectra of $CsPbBr_3$ nanocrystals obtained during the step increase of reaction temperature after seed nanocrystals were injected (prepared at <18 °C) at 50 °C. Dual absorption peaks for different confinements of nanocrystals could be clearly visible during transformation of one size/shape to another. In each case, the size and thickness of these nanocrystals are indicated near each spectrum. Figure 3b shows the corresponding PL spectra of these nanocrystals, which also showed the dual nature in the transition (or mixed) states. However, after 3.0 nm, only cubes were formed and their size also increased with the increase of reaction temperature. Three representative TEM images obtained from intermediate samples

https://doi.org/10.1021/acsphyschemau.2c00001
ACS Phys. Chem Au 2022, 2, 268–276

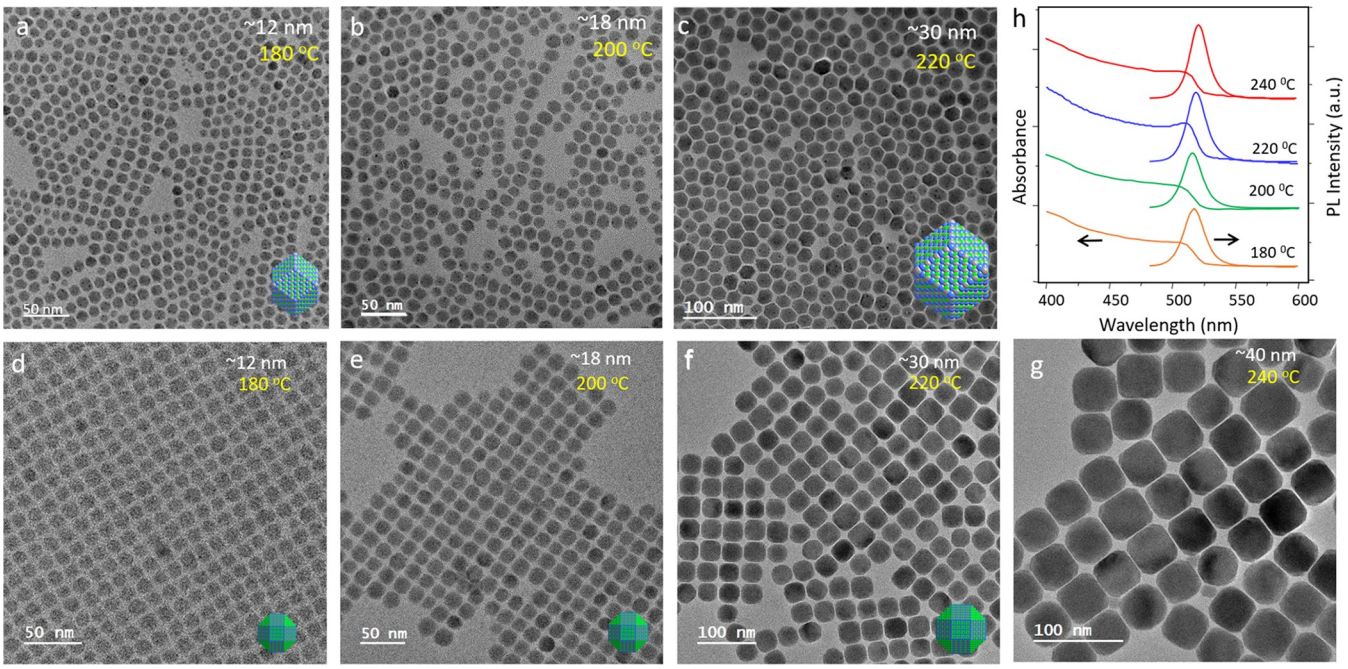

Figure 4. Size-tunable $CsPbBr_3$ nanocrystals beyond the quantum confinement regime and obtained from one size for one temperature reactions. TEM images of dodecahedron nanocrystals obtained at (a) 180, (b) 200, and (c) 220 °C reactions. TEM images of rhombicuboctahedron-shaped nanocrystals obtained at (d) 180, (e) 200, (f) 220, and (g) 240 °C. (h) Absorption and PL spectra of polyhedron nanocrystals. Reproduced from ref 31. Copyright 2020 American Chemical Society.

are presented in Figure 3c–e, and these confirmed that the shape also varied from one dimension to another during annealing.

Analysis of these transformations clearly demonstrated that thermodynamic equilibrium can lead to interconversion of perovskite nanocrystals from smaller to larger dimensions. This has been explained as Ostwald ripening but does not exactly follow the ripening mechanism. Moreover, there is no evidence on material transfer via solution from one particle to another nor any proof on how the shape from platelets to cubes or even cubes to larger size cubes was transformed. Certainly, more evidence needs to be collected, though the confirmed growth could be possible in one reaction with progress of the reaction time along with increase of reaction temperature. Unfortunately, this also could not establish the kinetic control of nanocrystal growth, retaining a fixed number of nucleations and its original shape, as established for the classical mechanism.

Apart from these standard cube shapes, size variations of other recently reported polyhedral shapes of nanocrystals using different ligands and reagents were also investigated.[31] Figure 4 presents 12 faceted rhombic dodecahedron nanocrystals (Figure 4a–c) and 26 faceted rhombicuboctahedron nanocrystals (Figure 4d–g) ranging from ∼12 to >40 nm diameter. All of these nanocrystals were obtained using phenacyl bromide as the halide reagents and with injection of the Cs(I) precursor at different reaction temperatures. Like the cube structures, herein, also the size increased with an increase of the reaction temperature. Initially, dodecahedron nanocrystals were formed, and with continuous annealing, their vertices were dissolved and became rhombicuboctahedron shapes.[31] However, at higher temperature of 240 °C, only the final nanostructures could be trapped. Figure 4h presents the absorption and photoluminescence spectra of these nanocrystals obtained at different reaction temperatures, and all showed almost similar nature as that of bulk $CsPbBr_3$. However, excited-state decay lifetimes of these nanocrystals were reported to be longer than those of traditional cube nanocrystals.

These results, which showed the size-tunable $CsPbBr_3$ nanocrystals in a wider size regime and beyond the quantum confinements, also followed the one reaction for one size principle. These also showed the thermodynamic control principle in which size remained directly proportional to the respective reaction temperature. However, unfortunately, this could not help in establishing the growth kinetics of nanocrystals from one size to another in a same reaction. Here, thermal annealing changed the shape but could not increase the size. Hence, these results also remained ineffective for establishing both nucleations and growth of $CsPbBr_3$ nanocrystals in two different shapes and even in larger sizes of $CsPbBr_3$ perovskite nanocrystals.

Similar to the method for cube and polyhedral nanocrystals, a similar one reaction for one size principle was also reported for platelet formations. Reducing the reaction temperature reported by Kovalenko and co-workers,[1] Yang and co-workers[41] reported monolayer thickness-tunable platelets at reaction temperatures of 90–130 °C. Figure 5a presents typical absorption and PL spectra of these thickness-tunable platelets from 1 unit to 5 unit cells. The formation principle here was similar to that of thermodynamically controlled nanocubes and polyhedron-shaped nanocrystals. Further, Bohn et al.[13] reported similar thickness-tunable platelets with Cs(I) to Pb(II) concentration variations at a fixed reaction temperature (Figure 5b). Even though the temperature here was not varied, nanoplatelets were formed following the principle of one size from one reaction, in which growth kinetics could not be established.

Apart from the above reports on one size from one reaction, successes have also been achieved obtaining size-tunable nanocrystals in one reaction. Manna and co-workers reported alkyl phosphonic acid as an ideal reagent for obtaining size-tunable truncated cube-shaped $CsPbBr_3$ nanocrystals with

https://doi.org/10.1021/acsphyschemau.2c00001
ACS Phys. Chem Au 2022, 2, 268–276

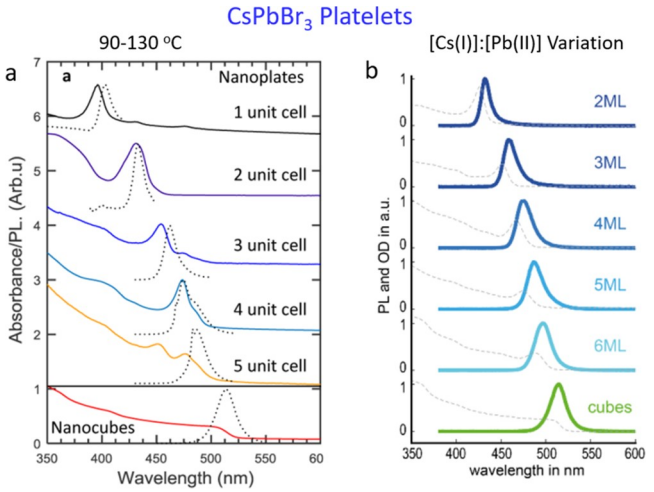

Figure 5. (a) Absorption and corresponding PL spectra of $CsPbBr_3$ platelets obtained with temperature variations. Reproduced from ref 41. Copyright 2015 American Chemical Society. (b) Absorption and corresponding PL spectra of $CsPbBr_3$ platelets obtained with Cs(I) to Pb(II) concentration variations. Reproduced from ref 13. Copyright 2018 American Chemical Society.

progress of the reaction.[42] At 100 °C, they could achieve three different sizes of $CsPbBr_3$ within a short annealing span using oleylphosphonic acid as the additional reagent. Though this was not the main focus in the report, this is a straightforward result for obtaining growth kinetics of these nanocrystals. A model of a phosphonic-acid-capped nanocrystal is shown in Figure 6a. Typical absorption and PL spectra obtained for tunable nanocrystals are depicted in the bottom panel of Figure 6a. Further, Mathews and co-workers reported a similar reaction at room temperature using short chain octyl phosphonic acid, and they could successfully achieve size-tunable nanocrystals in a single reaction.[39] Absorption and PL spectra obtained from 30 to 2400 s are presented in Figure 6b,c, respectively. Nanocrystal diameter with reaction time and respective PL quantum yields are further provided in Figure 6d. In this case, the time period could be seen beyond a standard reaction time scale, and the shapes of these nanocrystals varied during annealing. Hence, these results provided straightforward kinetics data during formation of $CsPbBr_3$ nanocrystals in a single reaction. However, more optimization and particularly high temperature synthesis leading to successful size tunability with unaltered shape within a permittable reaction scale are required for establishing kinetics models of the formation of these nanocrystals.

For typical covalent nanocrystals like in metal chalcogenides, their growth mechanism is widely established. La Mer plots mostly provide the relation of monomer concentration with the evolutions of nanocrystals in the progress of the reaction.[33] At the critical limiting supersaturation stage, nucleations were formed and then growth continued with diffusion of ions. This is typically defined in three stages of reaction, as depicted in Figure 7a. More details of the formation of nanocrystals are further provided in Figure 7b, in which nucleations, growth, and Ostwald ripening stages with progress of reaction time are

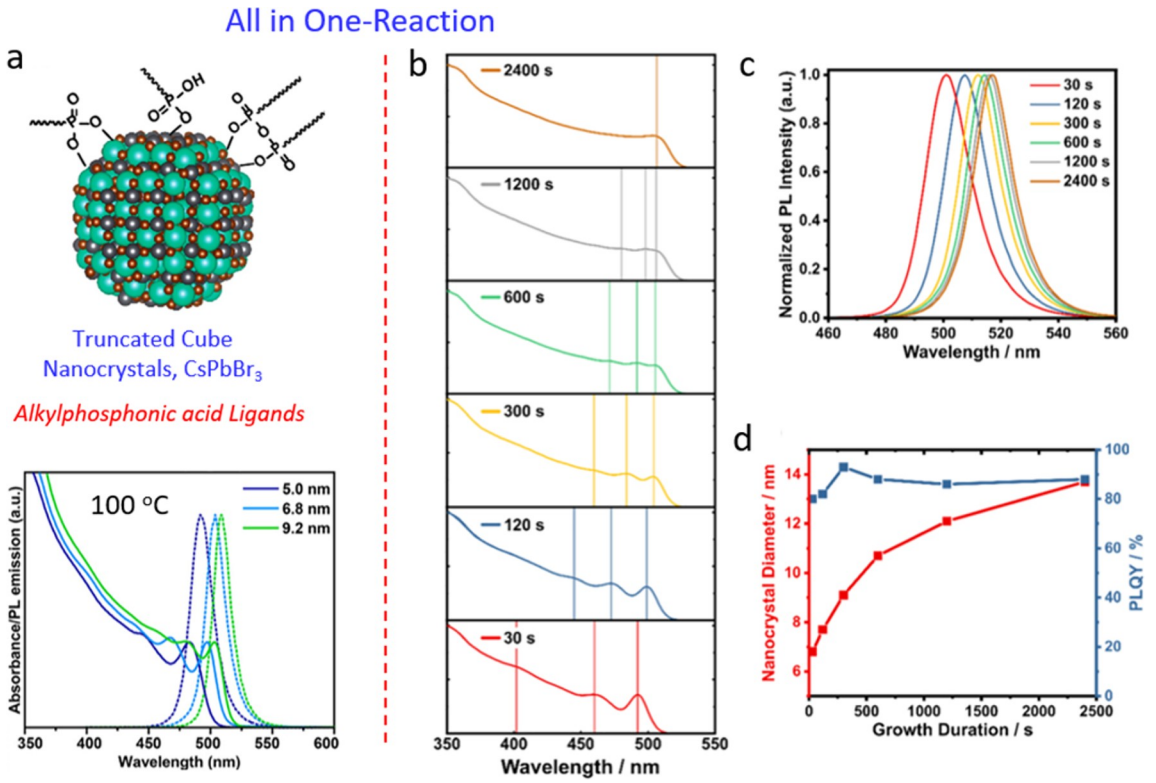

Figure 6. (a) Model of alkyl phosphonic acid-capped truncated cube-shaped $CsPbBr_3$ nanocrystal, with the bottom image showing the absorption and PL spectra of size-tunable nanocrystals obtained at 100 °C. Reproduced from ref 42. Copyright 2020 American Chemical Society. (b) Absorption and (c) corresponding PL spectra of $CsPbBr_3$ nanocrystals obtained using octylphosphonic acid at room temperature. Reaction time in each case has been marked in each panel. (d) Plots of size of nanocrystals and PLQY with growth durations of $CsPbBr_3$ nanocrystals. Reproduced from ref 39. Copyright 2021 American Chemical Society.

https://doi.org/10.1021/acsphyschemau.2c00001
ACS Phys. Chem Au 2022, 2, 268−276

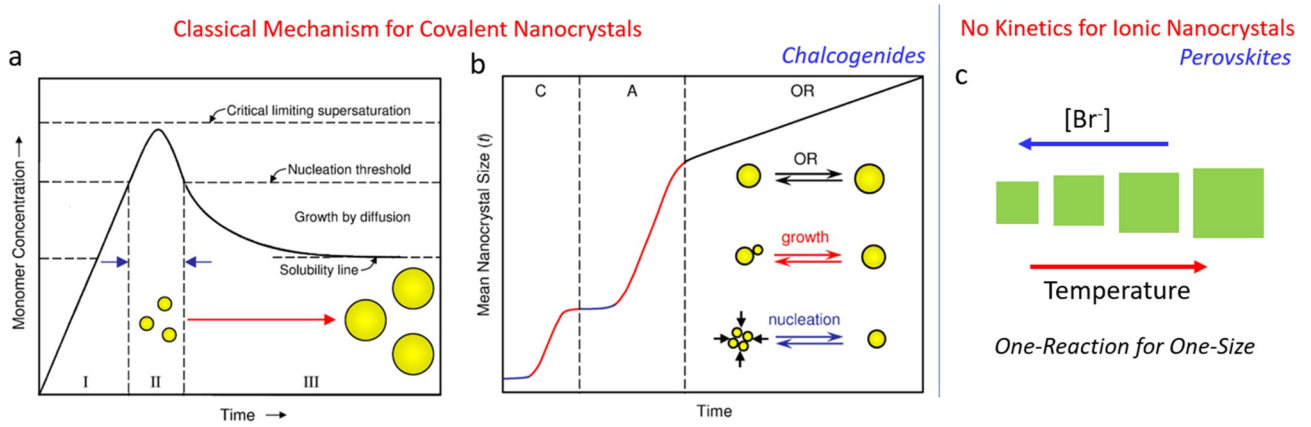

Figure 7. (a) La Mer reaction model of formation of nucleation and growth of nanocrystals in solution. Blue and red arrows signify nucleation and growth controls, respectively. (b) Reaction kinetics for size evolution of nanocrystals from nucleation to achieving the desired size. Reproduced from ref 33. Copyright 2014 American Chemical Society. (c) Schematics of size variation for ionic-type perovskite nanocrystals with halide and temperature variations.

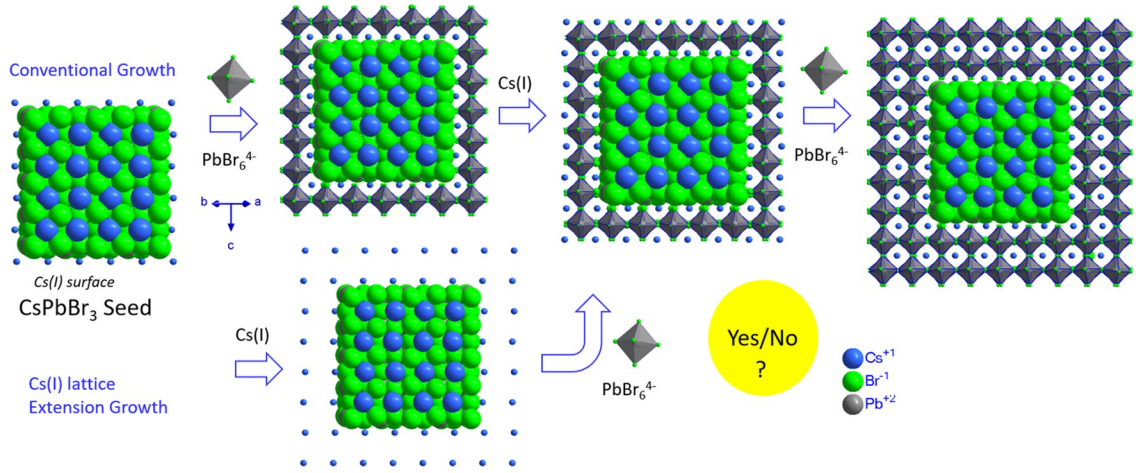

Figure 8. Schematics of atomic models showing growths of $CsPbBr_3$ nanocrystals with alternative positive and negative ion adsorption and reaction and Cs lattice extension models.

correlated. These plots are only valid when the crystal growth follows the kinetically controlled process. Unfortunately, as stated, almost all perovskite syntheses do not provide any avenue for their growth with reaction time. Summarizing all of these synthesis processes with either precursor variation or reaction temperature (Figure 7c), it can be concluded that instantaneous formation of these nanocrystals truly hindered deriving the reaction kinetics, and this is possibly because of their ionic nature.

Hence, the question arises whether growth kinetics of formation of lead halide perovskite nanocrystals can be formulated or not? In solution, formation processes of all crystals should follow both nucleation and growth processes as well as for perovskite nanocrystals. As decoupling of growth from nucleation remains a major hurdle, establishing secondary growth including core/shell or heterostructure formation remains indeed difficult. However, the reaction model with alkyl phosphonic acid reagents provides hope for slowing down the reaction process, and this might a step forward for deriving kinetics of nanocrystal growth. It was also possible that, while smaller size particles were injected into the reaction system at a higher reaction temperature, these became larger-sized and this phenomenon further relies on material transfer and a change in density of the particles during the progress of the reactions. Hence, growth of these nanocrystals could certainly be possible, but this needs a proper strategy to design the chemical reaction.

Further, the question arises how to control this growth. This remained indeed a major challenge, and as stated in the introduction, despite large successes in obtaining highly emitting perovskite nanocrystals, the stepwise or successive growth could not be established. The successful and conventional growth for covalent nanocrystals adopt mostly the simultaneous ion adsorption and reaction approach. Accordingly, for $CsPbBr_3$ nanocrystals, the model is proposed (Figure 8), in which surface-rich Cs(I) nanocrystals were allowed to react with $PbBr_6^{4-}$ octahedra and then again with Cs(I) followed by $PbBr_6^{4-}$ octahedra to create monolayers on seed nanocrystals. However, this looks ideal in designing, but indeed, it was difficult to perform in reaction flasks. Instead, the model worked partially with Cs sublattice extension,[43,44] which is depicted in Figure 8. In this case, it was successful for one or two facets of seed cubes but failed in shelling the entire surface of the cubes. These results suggest that there is hope of shelling or inducing secondary growth with the same material or with a different formation of the desired core/shell nanocrystals. However, this requires control of growth kinetics, and unless the growth is

https://doi.org/10.1021/acsphyschemau.2c00001
ACS Phys. Chem Au 2022, 2, 268−276

decoupled from nucleations and monitored with progress of the reaction, inducing secondary nucleations and performing further growth truly remains difficult.

Common parameters to control such reactions are (1) reaction temperature, (2) nature of A-site Cs(I) and B-site Pb(II) precursors, (3) halide precursor, (4) amine/acid equilibria for controlling precursor reactivity and surface binding, (5) specially designed ligands, (6) surface-terminating sites for A-site ligand binding or with Pb(II), and (7) new controlling additive for slowing down reactivity but not binding to final nanocrystals. Significant research already has progressed in varying these parameters,[13,38,39,42,45−−60] but none of the cases provided solid evidence of the kinetic model of crystal growth at constant reaction temperature and without adding any additional size-controlling reagent. Hence, certainly, more reagents need to be searched or designed to slow down the reaction process and cease the growth of these nanocrystals.

In summary, different reactions optimized for size variations of $CsPbBr_3$ perovskite nanocrystals were studied, and their controlling parameters were analyzed. In most cases, the one reaction for one size model was adopted with variation of reaction temperature or concentration of halides or other precursors. In addition, though not widely explored, different size particles from one reaction with progress of the reaction and increase of temperature were also investigated. However, in neither case, there is clear evidence of growth kinetics leading to size tunability from one size regime to another was achieved. The major hurdle for obtaining such control remains with their fast reaction and difficulty in decoupling growths from nucleations. The possible reason for this could be the ionic nature of lead halide perovskite nanocrystals. However, as different facets were tuned and armed nanostructures were already reported, it is expected that controlling growth and establishing kinetic models for these solution-processed nanocrystals could soon be possible. However, at this point, it can be stated here that the growth of lead halide perovskite nanocrystals still remains a mystery, and both theoretical and experimental advances are required for solving the same.

AUTHOR INFORMATION

Corresponding Author

Narayan Pradhan − *School of Materials Sciences, Indian Association for the Cultivation of Science, Kolkata 700032, India;* orcid.org/0000-0003-4646-8488; Email: camnp@iacs.res.in

Complete contact information is available at: https://pubs.acs.org/10.1021/acsphyschemau.2c00001

Notes

The author declares no competing financial interest.

Biography

Narayan Pradhan is currently working as a Professor in the School of Materials Sciences at the Indian Association for the Cultivation of Science at Kolkata, India. He obtained a Ph.D. degree from IIT Kharagpur and continued post docs in Israel and the USA. His current works focus on developing facet chemistry of lead halide perovskites and their shape tuning.

ACKNOWLEDGMENTS

This work was a part of proposed research work of the proposal no. DST/NM/NS/2019/324 sanctioned by DST Nanomission.

REFERENCES

(1) Protesescu, L.; Yakunin, S.; Bodnarchuk, M. I.; Krieg, F.; Caputo, R.; Hendon, C. H.; Yang, R. X.; Walsh, A.; Kovalenko, M. V. Nanocrystals of Cesium Lead Halide Perovskites ($CsPbX_3$, X = Cl, Br, and I): Novel Optoelectronic Materials Showing Bright Emission with Wide Color Gamut. *Nano Lett.* **2015**, *15*, 3692−3696.

(2) Shamsi, J.; Urban, A. S.; Imran, M.; De Trizio, L.; Manna, L. Metal Halide Perovskite Nanocrystals: Synthesis, Post-Synthesis Modifications, and Their Optical Properties. *Chem. Rev.* **2019**, *119*, 3296−3348.

(3) Dey, A.; Ye, J.; De, A.; Debroye, E.; Ha, S. K.; Bladt, E.; Kshirsagar, A. S.; Wang, Z.; Yin, J.; Wang, Y.; et al. State of the Art and Prospects for Halide Perovskite Nanocrystals. *ACS Nano* **2021**, *15*, 10775−10981.

(4) Pradhan, N. Alkylammonium Halides for Facet Reconstruction and Shape Modulation in Lead Halide Perovskite Nanocrystals. *Acc. Chem. Res.* **2021**, *54*, 1200−1208.

(5) Kazes, M.; Udayabhaskararao, T.; Dey, S.; Oron, D. Effect of Surface Ligands in Perovskite Nanocrystals: Extending in and Reaching out. *Acc. Chem. Res.* **2021**, *54*, 1409−1418.

(6) Wei, Y.; Cheng, Z.; Lin, J. An Overview on Enhancing the Stability of Lead Halide Perovskite Quantum Dots and Their Applications in Phosphor-converted LEDs. *Chem. Soc. Rev.* **2019**, *48*, 310−350.

(7) Pradhan, N. Why Do Perovskite Nanocrystals Form Nanocubes and How Can Their Facets Be Tuned? A Perspective from Synthetic Prospects. *ACS Energy Lett.* **2021**, *6*, 92−99.

(8) Huang, H.; Bodnarchuk, M. I.; Kershaw, S. V.; Kovalenko, M. V.; Rogach, A. L. Lead Halide Perovskite Nanocrystals in the Research Spotlight: Stability and Defect Tolerance. *ACS Energy Lett.* **2017**, *2*, 2071−2083.

(9) Imran, M.; Caligiuri, V.; Wang, M.; Goldoni, L.; Prato, M.; Krahne, R.; De Trizio, L.; Manna, L. Benzoyl Halides as Alternative Precursors for the Colloidal Synthesis of Lead-Based Halide Perovskite Nanocrystals. *J. Am. Chem. Soc.* **2018**, *140*, 2656−2664.

(10) Shamsi, J.; Dang, Z.; Ijaz, P.; Abdelhady, A. L.; Bertoni, G.; Moreels, I.; Manna, L. Colloidal CsX (X = Cl, Br, I) Nanocrystals and Their Transformation to $CsPbX_3$ Nanocrystals by Cation Exchange. *Chem. Mater.* **2018**, *30*, 79−83.

(11) Dong, Y.; Qiao, T.; Kim, D.; Parobek, D.; Rossi, D.; Son, D. H. Precise Control of Quantum Confinement in Cesium Lead Halide Perovskite Quantum Dots via Thermodynamic Equilibrium. *Nano Lett.* **2018**, *18*, 3716−3722.

(12) Dutta, A.; Behera, R. K.; Pal, P.; Baitalik, S.; Pradhan, N. Near-Unity Photoluminescence Quantum Efficiency for All $CsPbX_3$ (X = Cl, Br, and I) Perovskite Nanocrystals: A Generic Synthesis Approach. *Angew. Chem., Int. Ed.* **2019**, *58*, 5552−5556.

(13) Bohn, B. J.; Tong, Y.; Gramlich, M.; Lai, M. L.; Doeblinger, M.; Wang, K.; Hoye, R. L. Z.; Mueller-Buschbaum, P.; Stranks, S. D.; Urban, A. S.; Polavarapu, L.; Feldmann, J. Boosting Tunable Blue Luminescence of Halide Perovskite Nanoplatelets through Postsynthetic Surface Trap Repair. *Nano Lett.* **2018**, *18*, 5231−5238.

(14) Zheng, X.; Hou, Y.; Sun, H.-T.; Mohammed, O. F.; Sargent, E. H.; Bakr, O. M. Reducing Defects in Halide Perovskite Nanocrystals for Light-Emitting Applications. *J. Phys. Chem. Lett.* **2019**, *10*, 2629−2640.

(15) Pan, J.; Shang, Y.; Yin, J.; De Bastiani, M.; Peng, W.; Dursun, I.; Sinatra, L.; El-Zohry, A. M.; Hedhili, M. N.; Emwas, A.-H.; et al. Bidentate Ligand-Passivated $CsPbI_3$ Perovskite Nanocrystals for Stable Near-Unity Photoluminescence Quantum Yield and Efficient Red Light-Emitting Diodes. *J. Am. Chem. Soc.* **2018**, *140*, 562−565.

(16) Pan, J.; Quan, L. N.; Zhao, Y.; Peng, W.; Murali, B.; Sarmah, S. P.; Yuan, M.; Sinatra, L.; Alyami, N. M.; Liu, J.; et al. Highly Efficient Perovskite-Quantum-Dot Light-Emitting Diodes by Surface Engineering. *Adv. Mater.* **2016**, *28*, 8718−8725.

(17) Zheng, X.; Yuan, S.; Liu, J.; Yin, J.; Yuan, F.; Shen, W.-S.; Yao, K.; Wei, M.; Zhou, C.; Song, K.; et al. Chlorine Vacancy Passivation in Mixed Halide Perovskite Quantum Dots by Organic Pseudohalides Enables Efficient Rec. 2020 Blue Light-Emitting Diodes. *ACS Energy Lett.* **2020**, *5*, 793−798.

(18) Ahmed, T.; Seth, S.; Samanta, A. Boosting the Photoluminescence of $CsPbX_3$ (X = Cl, Br, I) Perovskite Nanocrystals

Covering a Wide Wavelength Range by Postsynthetic Treatment with Tetrafluoroborate Salts. *Chem. Mater.* **2018**, *30*, 3633−3637.
(19) Paul, S.; Samanta, A. N-Bromosuccinimide as Bromide Precursor for Direct Synthesis of Stable and Highly Luminescent Green-Emitting Perovskite Nanocrystals. *ACS Energy Lett.* **2020**, *5*, 64−69.
(20) Mondal, N.; De, A.; Samanta, A. Achieving Near-Unity Photoluminescence Efficiency for Blue-Violet-Emitting Perovskite Nanocrystals. *ACS Energy Lett.* **2019**, *4*, 32−39.
(21) Dutta, A.; Behera, R. K.; Dutta, S. K.; Das Adhikari, S.; Pradhan, N. Annealing $CsPbX_3$ (X = Cl and Br) Perovskite Nanocrystals at High Reaction Temperatures: Phase Change and Its Prevention. *J. Phys. Chem. Lett.* **2018**, *9*, 6599−6604.
(22) Dutta, A.; Dutta, S. K.; Das Adhikari, S.; Pradhan, N. Phase-Stable $CsPbI_3$ Nanocrystals: The Reaction Temperature Matters. *Angew. Chem., Int. Ed.* **2018**, *57*, 9083−9087.
(23) Pradhan, N. Tips and Twists in Making High Photoluminescence Quantum Yield Perovskite Nanocrystals. *ACS Energy Lett.* **2019**, *4*, 1634−1638.
(24) Dutta, A.; Pradhan, N. Phase-Stable Red-Emitting $CsPbI_3$ Nanocrystals: Successes and Challenges. *ACS Energy Lett.* **2019**, *4*, 709−719.
(25) Zhang, B.; Goldoni, L.; Zito, J.; Dang, Z.; Almeida, G.; Zaccaria, F.; de Wit, J.; Infante, I.; De Trizio, L.; Manna, L. Alkyl Phosphonic Acids Deliver $CsPbBr_3$ Nanocrystals with High Photoluminescence Quantum Yield and Truncated Octahedron Shape. *Chem. Mater.* **2019**, *31*, 9140−9147.
(26) Akkerman, Q. A.; Meggiolaro, D.; Dang, Z.; De Angelis, F.; Manna, L. Fluorescent Alloy $CsPb_xMn_{1-x}I_3$ Perovskite Nanocrystals with High Structural and Optical Stability. *ACS Energy Lett.* **2017**, *2*, 2183−2186.
(27) Almeida, G.; Goldoni, L.; Akkerman, Q.; Dang, Z.; Khan, A. H.; Marras, S.; Moreels, I.; Manna, L. Role of Acid-Base Equilibria in the Size, Shape, and Phase Control of Cesium Lead Bromide Nanocrystals. *ACS Nano* **2018**, *12*, 1704−1711.
(28) Akkerman, Q. A.; Accornero, S.; Scarpellini, A.; Prato, M.; Manna, L.; D'Innocenzo, V.; Petrozza, A. Tuning the Optical Properties of Cesium Lead Halide Perovskite Nanocrystals by Anion Exchange Reactions. *J. Am. Chem. Soc.* **2015**, *137*, 10276−81.
(29) Parobek, D.; Dong, Y.; Qiao, T.; Rossi, D.; Son, D. H. Photoinduced Anion Exchange in Cesium Lead Halide Perovskite Nanocrystals. *J. Am. Chem. Soc.* **2017**, *139*, 4358−4361.
(30) Otero-Martínez, C.; García-Lojo, D.; Pastoriza-Santos, I.; Pérez-Juste, J.; Polavarapu, L. Dimensionality Control of Inorganic and Hybrid Perovskite Nanocrystals by Reaction Temperature: From No-Confinement to 3D and 1D Quantum Confinement. *Angew. Chem., Int. Ed.* **2021**, *60*, 26677−26684.
(31) Bera, S.; Behera, R. K.; Pradhan, N. α-Halo Ketone for Polyhedral Perovskite Nanocrystals: Evolutions, Shape Conversions, Ligand Chemistry, and Self-Assembly. *J. Am. Chem. Soc.* **2020**, *142*, 20865−20874.
(32) Hudait, B.; Dutta, S. K.; Pradhan, N. Isotropic $CsPbBr_3$ Perovskite Nanocrystals beyond Nanocubes: Growth and Optical Properties. *ACS Energy Lett.* **2020**, *5*, 650−656.
(33) Wang, F.; Richards, V. N.; Shields, S. P.; Buhro, W. E. Kinetics and Mechanisms of Aggregative Nanocrystal Growth. *Chem. Mater.* **2014**, *26*, 5−21.
(34) Dutta, A.; Dutta, S. K.; Das Adhikari, S.; Pradhan, N. Tuning the Size of $CsPbBr_3$ Nanocrystals: All at One Constant Temperature. *ACS Energy Lett.* **2018**, *3*, 329−334.
(35) Akkerman, Q. A.; Motti, S. G.; Srimath Kandada, A. R.; Mosconi, E.; D'Innocenzo, V.; Bertoni, G.; Marras, S.; Kamino, B. A.; Miranda, L.; De Angelis, F.; Petrozza, A.; Prato, M.; Manna, L.; et al. Solution Synthesis Approach to Colloidal Cesium Lead Halide Perovskite Nanoplatelets with Monolayer-Level Thickness Control. *J. Am. Chem. Soc.* **2016**, *138*, 1010−1016.
(36) Huang, H.; Feil, M. W.; Fuchs, S.; Debnath, T.; Richter, A. F.; Tong, Y.; Wu, L.; Wang, Y.; Döblinger, M.; Nickel, B. Growth of Perovskite $CsPbBr_3$ Nanocrystals and Their Formed Superstructures Revealed by In Situ Spectroscopy. *Chem. Mater.* **2020**, *32*, 8877−8884.
(37) Wen, J.-R.; Roman, B. J.; Rodriguez Ortiz, F. A.; Mireles Villegas, N.; Porcellino, N.; Sheldon, M. Chemical Availability of Bromide Dictates $CsPbBr_3$ Nanocrystal Growth. *Chem. Mater.* **2019**, *31*, 8551−8557.
(38) Leng, J.; Wang, T.; Zhao, X.; Ong, E. W. Y.; Zhu, B.; Ng, J. D. A.; Wong, Y.-C.; Khoo, K. H.; Tamada, K.; Tan, Z.-K. Thermodynamic Control in the Synthesis of Quantum-Confined Blue-Emitting $CsPbBr_3$ Perovskite Nanostrips. *J. Phys. Chem. Lett.* **2020**, *11*, 2036−2043.
(39) Brown, A. M.; Vashishtha, P.; Hooper, T. J. N.; Ng, Y. F.; Nutan, G. V.; Fang, Y.; Giovanni, D.; Tey, J. N.; Jiang, L.; Damodaran, B.; et al. Precise Control of $CsPbBr_3$ Perovskite Nanocrystal Growth at Room Temperature: Size Tunability and Synthetic Insights. *Chem. Mater.* **2021**, *33*, 2387−2397.
(40) Peng, L.; Dutta, A.; Xie, R.; Yang, W.; Pradhan, N. Dot−Wire−Platelet−Cube: Step Growth and Structural Transformations in $CsPbBr_3$ Perovskite Nanocrystals. *ACS Energy Lett.* **2018**, *3*, 2014−2020.
(41) Bekenstein, Y.; Koscher, B. A.; Eaton, S. W.; Yang, P.; Alivisatos, A. P. Highly Luminescent Colloidal Nanoplates of Perovskite Cesium Lead Halide and Their Oriented Assemblies. *J. Am. Chem. Soc.* **2015**, *137*, 16008−16011.
(42) Zhang, B.; Goldoni, L.; Lambruschini, C.; Moni, L.; Imran, M.; Pianetti, A.; Pinchetti, V.; Brovelli, S.; De Trizio, L.; Manna, L. Stable and Size Tunable $CsPbBr_3$ Nanocrystals Synthesized with Oleylphosphonic Acid. *Nano Lett.* **2020**, *20*, 8847−8853.
(43) Dutta, S. K.; Bera, S.; Behera, R. K.; Hudait, B.; Pradhan, N. Cs-Lattice Extension and Expansion for Inducing Secondary Growth of $CsPbBr_3$ Perovskite Nanocrystals. *ACS Nano* **2021**, *15*, 16183−16193.
(44) Dutta, S. K.; Bera, S.; Pradhan, N. Why Is Making Epitaxially Grown All Inorganic Perovskite−Chalcogenide Nanocrystal Heterostructures Challenging? Some Facts and Some Strategies. *Chem. Mater.* **2021**, *33*, 3868−3877.
(45) Zhao, J.; Cao, S.; Li, Z.; Ma, N. Amino Acid-Mediated Synthesis of $CsPbBr_3$ Perovskite Nanoplatelets with Tunable Thickness and Optical Properties. *Chem. Mater.* **2018**, *30*, 6737−6743.
(46) Wang, T.; Yang, Z.; Yang, L.; Yu, X.; Sun, L.; Qiu, J.; Zhou, D.; Lu, W.; Yu, S. F.; Lin, Y.; Xu, X. Atomic-Scale Insights into the Dynamics of Growth and Degradation of All-Inorganic Perovskite Nanocrystals. *J. Phys. Chem. Lett.* **2020**, *11*, 4618−4624.
(47) Le, T.-H.; Lee, S.; Jo, H.; Jeong, G.; Chang, M.; Yoon, H. Morphology-Dependent Ambient-Condition Growth of Perovskite Nanocrystals for Enhanced Stability in Photoconversion Device. *J. Phys. Chem. Lett.* **2021**, *12*, 5631−5638.
(48) Bera, S.; Behera, R. K.; Das Adhikari, S.; Guria, A. K.; Pradhan, N. Equilibriums in Formation of Lead Halide Perovskite Nanocrystals. *J. Phys. Chem. Lett.* **2021**, *12*, 11824−11833.
(49) Xu, L.-J.; Worku, M.; He, Q.; Lin, H.; Zhou, C.; Chen, B.; Lin, X.; Xin, Y.; Ma, B. Ligand-Mediated Release of Halides for Color Tuning of Perovskite Nanocrystals with Enhanced Stability. *J. Phys. Chem. Lett.* **2019**, *10*, 5836−5840.
(50) Imran, M.; Ijaz, P.; Baranov, D.; Goldoni, L.; Petralanda, U.; Akkerman, Q.; Abdelhady, A. L.; Prato, M.; Bianchini, P.; Infante, I.; Manna, L. Shape-Pure, Nearly Monodispersed $CsPbBr_3$ Nanocubes Prepared Using Secondary Aliphatic Amines. *Nano Lett.* **2018**, *18*, 7822−7831.
(51) Das, S.; De, A.; Samanta, A. Ambient Condition Mg^{2+} Doping Producing Highly Luminescent Green- and Violet-Emitting Perovskite Nanocrystals with Reduced Toxicity and Enhanced Stability. *J. Phys. Chem. Lett.* **2020**, *11*, 1178−1188.
(52) Shamsi, J.; Dang, Z.; Bianchini, P.; Canale, C.; Di Stasio, F.; Brescia, R.; Prato, M.; Manna, L. Colloidal Synthesis of Quantum Confined Single Crystal $CsPbBr_3$ Nanosheets with Lateral Size Control up to the Micrometer Range. *J. Am. Chem. Soc.* **2016**, *138*, 7240−7243.
(53) Koscher, B. A.; Swabeck, J. K.; Bronstein, N. D.; Alivisatos, A. P. Essentially Trap-Free $CsPbBr_3$ Colloidal Nanocrystals by Postsynthetic Thiocyanate Surface Treatment. *J. Am. Chem. Soc.* **2017**, *139*, 6566−6569.
(54) Koscher, B. A.; Bronstein, N. D.; Olshansky, J. H.; Bekenstein, Y.; Alivisatos, A. P. Surface- vs. Diffusion-Limited Mechanisms of Anion

Exchange in $CsPbBr_3$ Nanocrystal Cubes Revealed through Kinetic Studies. *J. Am. Chem. Soc.* **2016**, *138*, 12065−12068.
(55) Balakrishnan, S. K.; Kamat, P. V. Ligand Assisted Transformation of Cubic $CsPbBr_3$ Nanocrystals into Two-Dimensional $CsPb_2Br_5$ Nanosheets. *Chem. Mater.* **2018**, *30*, 74−78.
(56) Huang, H.; Xue, Q.; Chen, B.; Xiong, Y.; Schneider, J.; Zhi, C.; Zhong, H.; Rogach, A. L. Top-Down Fabrication of Stable Methylammonium Lead Halide Perovskite Nanocrystals by Employing a Mixture of Ligands as Coordinating Solvents. *Angew. Chem., Int. Ed.* **2017**, *56*, 9571−9576.
(57) Ravi, V. K.; Santra, P. K.; Joshi, N.; Chugh, J.; Singh, S. K.; Rensmo, H.; Ghosh, P.; Nag, A. Origin of Substitution Mechanism for Binding of Organic Ligands on Surface of $CsPbBr_3$ Perovskite Nanocubes. *J. Phys. Chem. Lett.* **2017**, *8*, 4988−4994.
(58) Swarnkar, A.; Chulliyil, R.; Ravi, V. K.; Irfanullah, M.; Chowdhury, A.; Nag, A. Colloidal $CsPbBr_3$ Perovskite Nanocrystals: Luminescence beyond Traditional Quantum Dots. *Angew. Chem., Int. Ed.* **2015**, *54*, 15424−15428.
(59) Swarnkar, A.; Mir, W. J.; Nag, A. Can B-Site Doping or Alloying Improve Thermal- and Phase-Stability of All-Inorganic $CsPbX_3$ (X = Cl, Br, I) Perovskites? *ACS Energy Lett.* **2018**, *3*, 286−289.
(60) Ravi, V. K.; Markad, G. B.; Nag, A. Band Edge Energies and Excitonic Transition Probabilities of Colloidal $CsPbX_3$ (X = Cl, Br, I) Perovskite Nanocrystals. *ACS Energy Lett.* **2016**, *1*, 665−671.

https://doi.org/10.1021/acsphyschemau.2c00001
ACS Phys. Chem Au 2022, 2, 268−276